Title

Katanin-like protein Katnal2 is required for ciliogenesis and brain development in Xenopus embryos.

Journal

Developmental biology, 442(2)

ISSN

0012-1606

Authors

Willsey, Helen Rankin
Walentek, Peter
Exner, Cameron RT
et al.

Publication Date

2018-10-01

DOI

10.1016/j.ydbio.2018.08.002

Developmental Biology 442 (2018) 276–287

Contents lists available at ScienceDirect

Developmental Biology

journal homepage: www.elsevier.com/locate/developmentalbiology

Katanin-like protein Katnal2 is required for ciliogenesis and brain development in *Xenopus* embryos

Helen Rankin Willsey[b,c], Peter Walentek[b,1], Cameron R.T. Exner[c], Yuxiao Xu[b,c], Andrew B. Lane[b], Richard M. Harland[b], Rebecca Heald[b], Niovi Santama[a,*]

[a] Department of Biological Sciences, University of Cyprus, Cyprus
[b] Department of Molecular & Cell Biology, University of California, Berkeley, USA
[c] Department of Psychiatry, Weill Institute for Neurosciences, University of California, San Francisco, USA

ARTICLE INFO

Keywords:
Katnal2
Cilia
Neurogenesis
Autism
Katanin
Xenopus

ABSTRACT

Microtubule remodeling is critical for cellular and developmental processes underlying morphogenetic changes and for the formation of many subcellular structures. Katanins are conserved microtubule severing enzymes that are essential for spindle assembly, ciliogenesis, cell division, and cellular motility. We have recently shown that a related protein, Katanin-like 2 (KATNAL2), is similarly required for cytokinesis, cell cycle progression, and ciliogenesis in cultured mouse cells. However, its developmental expression pattern, localization, and *in vivo* role during organogenesis have yet to be characterized. Here, we used *Xenopus* embryos to reveal that Katnal2 (1) is expressed broadly in ciliated and neurogenic tissues throughout embryonic development; (2) is localized to basal bodies, ciliary axonemes, centrioles, and mitotic spindles; and (3) is required for ciliogenesis and brain development. Since human *KATNAL2* is a risk gene for autism spectrum disorders, our functional data suggest that *Xenopus* may be a relevant system for understanding the relationship of mutations in this gene to autism and the underlying molecular mechanisms of pathogenesis.

1. Introduction

Microtubules (MTs) are dynamic cytoskeletal polymers critical for the form and function of numerous subcellular structures, including spindles and cilia (Kapitein and Hoogenraad, 2015). One major class of MT-severing enzymes are Katanins, identified in all major phyla of Eukaryotes. They are hexameric ATPases of the AAA family that assemble on the MT lattice and through interactions with the C-terminus of β-tubulin exert mechanical strain that destabilizes and severs MT protofilaments (Hartman et al., 1998; Hartman and Vale, 1999; McNally and Vale, 1993). Thus, Katanins and Katanin-like proteins contribute to microtubule plasticity during assembly or re-organization of MT-built cellular structures by producing multiple short segments as seeds or by breaking down existing MTs, respectively. This is an essential step for mitotic and meiotic spindle assembly, for both extending and resorbing ciliary axonemes, for MT-based axonal elongation in neurons, for re-structuring interphase MTs during the cell cycle, and for underlying cellular locomotion in migrating cells (Dymek et al., 2004; Heald and Nogales, 2002; Loughlin et al., 2011; Roll-Mecak and McNally, 2010; Sharma et al., 2007).

Recent functional characterization of Katanin-like protein 2 (KATNAL2) in cultured mouse cells implicates its functional relevance for multiple MT-dependent cellular processes: knockdown of KATNAL2 results in defective ciliogenesis, inefficient cytokinesis, enlarged cellular and nuclear size, increased number of centrioles, formation of aberrant multipolar mitotic spindles, mitotic defects, chromosome bridges, multinucleated cells, increased MT acetylation, and an altered cell cycle (Ververis et al., 2016). Interestingly, both loss- and gain-of-function of KATNAL2 cause defective primary ciliogenesis upon serum-starvation, indicating a concentration-dependent role in the assembly and maintenance of ciliary axonemes. The same study also revealed interactions of KATNAL2 with NUBP1 and NUBP2 (MRP/MinD-type P-loop NTPases), which are integral components of centrioles, negative regulators of ciliogenesis, and are implicated in centriole duplication (Christodoulou et al., 2006; Kypri et al., 2014; Ververis et al., 2016). These findings also suggested that the ciliogenesis-promoting activity of KATNAL2 may be inhibited by interactions

* Correspondence to: Department of Biological Sciences, University of Cyprus, University Avenue 1, 1678 Nicosia, Cyprus.
E-mail addresses: peter.walentek@medizin.uni-freiburg.de (P. Walentek), santama@ucy.ac.cy (N. Santama).
[1] Current affiliation: Renal Division, Department of Medicine, University Freiburg Medical Center, and Center for Biological Systems Analysis (ZBSA), University of Freiburg, Freiburg, Germany.

https://doi.org/10.1016/j.ydbio.2018.08.002
Received 10 April 2018; Received in revised form 5 August 2018; Accepted 5 August 2018
Available online 08 August 2018
0012-1606/

with the NUBP proteins under cycling conditions. This is consistent with findings in *Xenopus* embryos, where Nubp1 is involved in motile and primary ciliogenesis (Ioannou et al., 2013). Furthermore, human KATNAL2 also localizes to ciliary axonemes when overexpressed in *Xenopus* (Tu et al., 2018). KATNAL2 was additionally found to be important for the proper formation of MT-based structures in differentiating germ cells during mouse spermatogenesis (Dunleavy et al., 2017).

Beyond these recent critical insights into the function of KATNAL2, in-depth *in vivo* characterization is still required to elucidate the role of this protein in vertebrate development and is of special interest in particular in the nervous system where katanin proteins are associated with human disease. For example, deletion of Katanin-like protein 1 (*KATNAL1)* is potentially associated with microcephaly and intellectual disability, and mouse models show abnormal ciliary motility in the ventricular ependymal cells of the brain (Banks et al., 2017; Bartholdi et al., 2014); mutations in the p80 subunit of Katanin (*KATNB1*) cause severe disruptions in cortical development and microlissencephaly (Hu et al., 2014; Mishra-Gorur et al., 2014); and, *KATNAL2* has been identified as a risk gene for autism spectrum disorders (ASD) in patient sequencing studies (Iossifov et al., 2014; Neale et al., 2012; O'Roak et al., 2012; Sanders et al., 2012; Stessman et al., 2017; Willsey et al., 2013). Despite its potential significance for human health, the molecular function of KATNAL2 in the development of the nervous system remains unresolved, and this is the first study to specifically address this question.

In this study, we used *Xenopus* embryos to functionally characterize Katnal2's developmental roles *in vivo*, including its involvement in vertebrate neural development. Our study revealed that Katnal2 was expressed in a wide array of ciliated and neural tissues throughout development, was localized to ciliary axonemes, basal bodies, centrioles, and spindles, and was required for ciliogenesis and correct brain development.

2. Materials and methods

2.1. Xenopus embryos

Xenopus laevis and *Xenopus tropicalis* embryos were obtained, cultured, and microinjected according to standard protocols (Sive et al., 2000) and in accordance with UC Berkeley and UCSF IACUC protocols. *In vitro* fertilizations were performed for both species; natural matings were also performed for *X. tropicalis* (Khokha et al., 2002). Animals were staged according to the standard table of development (Nieuwkoop and Faber, 1994). Embryos were microinjected with antisense morpholino oligonucleotides, CRISPR/Cas9 ribonucleoprotein, or *in vitro* transcribed mRNAs into blastomeres at the two- or four-cell stage (see below for details).

2.2. RNA extraction and RT-PCR

Total RNA was extracted from 15 *X. tropicalis* embryos for each developmental stage shown (Fig. S1) using the RNeasy Plus Mini Kit (Qiagen). cDNA was synthesized from 1 μg of RNA at each developmental stage using the SuperScript III First-Strand synthesis system (Invitrogen). Full-length *katnal2* transcripts were amplified by polymerase chain reaction using the Expand High-Fidelity system (Roche) from stage 3 cDNA with primers matching $^{5'}$ATGGAACTCTCCTACCAGGC$^{3'}$ (forward) and $^{5'}$CTACACAGACTCGAATTCCTTC$^{3'}$ (reverse). Products were T/A cloned individually into vector pC2.1-TOPO (Invitrogen) and verified by DNA sequencing (UC Berkeley DNA Sequencing Facility). Two distinct full-length *X. tropicalis katnal2* isoforms were submitted to Genbank and can be found under accession number MH036373 (larger isoform) and MH036374 (shorter isoform).

For assessment of *katnal2* expression during embryonic development, semi-quantitative RT-PCR was performed with the same amount of cDNA template derived from different developmental stages, resulting in diagnostic 780 and 660 basepair amplicons (primers: $^{5'}$ATGGAACTCTCCTACCAGGC$^{3'}$ and $^{5'}$GGTTCTGGAGATAAATATCCCTG$^{3'}$). Parallel diagnostic reactions were performed as references for normalization for transcripts encoding ribonuclease type III protein *drosha* ($^{5'}$TTACAGACCGCTGTTTGCTG$^{3'}$ and $^{5'}$TCAGGCCCATGCGCATATAG$^{3'}$) and survival of motor neuron 2 protein *smn2*, involved in the biogenesis of small nuclear ribonucleoproteins, ($^{5'}$AAGTAGCGTGTCTATGGCAG$^{3'}$ and $^{5'}$TATTTCCATCTTCCGACCAAAT$^{3'}$), both known to exhibit stable and continuous expression from early embryonic development up to the end of metamorphosis (Dhorne-Pollet et al., 2013).

2.3. Whole mount RNA In Situ hybridization

Digoxygenin-11-UTP-labeled RNA probes for *X. tropicalis katnal2* were synthesized *in vitro* from *Xenopus* Genome Collection IMAGE clone 7866710, Genbank BC125808.1 (Morin, 2006) using *Kpn*I restriction enzyme and T7 polymerase (antisense), and *Xho*I restriction enzyme and SP6 polymerase (sense). *X. tropicalis* embryos from stage 1–44 were stained with BM-Purple (11442074001, Sigma) after RNA *in situ* hybridization (Sive et al., 2000).

2.4. Antibodies

An affinity-purified goat antibody against recombinant mouse KATNAL2 (accession number LN831865) (Ververis et al., 2016) was used at 1:100 for *Xenopus* embryos or at 1:75 for XL177 cells. An affinity-purified rabbit antibody against recombinant mouse KATNAL2 (accession number LN831865) was custom-made by Davids Biotechnologie (Regensburg, Germany) and used at 1:100 for embryos and 1:200 for cells. A mouse monoclonal antibody (mab) against acetylated-tubulin (T6793, Sigma) was used at 1:700 for embryos and 1:500 for cells and a mab against α-tubulin (T5168, Sigma) was used at 1:5000 for cells. Mouse antibodies were used against β-tubulin (DSHB, E7, 1:100), PCNA (Life Technologies, PC10, 1:100), and poly-glutamylation (AdipoGen, 1:100). A rabbit antibody was used against vGLUT1 (Abcam, ab77822, 1:100). Primary antibodies were used in conjunction with appropriate fluorescently labeled Alexa-Fluor secondary antibodies (Thermo Fisher Scientific).

2.5. Whole mount immunofluorescence

Staged *X. tropicalis* and *laevis* embryos were processed for whole-mount immunofluorescence. Briefly, *X. tropicalis* embryos were fixed in 4% paraformaldehyde for 40 min at room temperature, bleached for 1 h under a light box in 5% formamide and 4% peroxide in PBS, permeabilized for 1 h in PBS with 0.1% Triton X-100 (PBT), and blocked for 1 h in PBS with 10% CAS-Block (Life Technologies). Embryos were incubated in primary antibody diluted in CAS-Block overnight at 4 °C. Then embryos were washed for 30 min with PBT, blocked again for 30 min, and incubated with secondary antibodies diluted in CAS-Block for 2 h at room temperature. Embryos were washed for 1 h with PBT and then 1 h in PBS, and mounted on glass slides with vacuum grease in Vecta-Shield mounting media with DAPI (Vector Laboratories). *X. laevis* embryos were stained as previously described (Walentek et al., 2016).

2.6. Xenopus XL177 cell line

X. laevis XL177 epithelial cells (a gift from Eric Karsenti, EMBL) were cultured in L15 Leibovitz medium with 15% v/v FCS, 2 mM glutamine and 50 U/mL of penicillin/streptomycin, and maintained at 25 °C in atmospheric conditions. For induction of primary ciliogenesis, cells were grown in media without serum for 24 h and sampled for immunofluorescence in parallel with cultures of cycling cells grown in media with serum.

2.7. Immunofluorescence in cells

XL177 cells were fixed on coverslips with 3.7% w/v paraformaldehyde in PHEM (30 mM Hepes, 65 mM Pipes, pH 6.9, 10 mM EGTA and 2 mM $MgCl_2$) for 10 min and permeabilized for 15 min with 0.5% v/v Triton X-100 in PHEM. Alternatively, cells were pre-extracted for 5 s with 0.05% v/v Triton X-100 before fixation with 3.7% w/v paraformaldehyde in PHEM. Immunolabeling was carried out as previously described (Christodoulou et al., 2006) and coverslips were mounted with Dako Fluorescent Mounting Medium (Dako, USA).

2.8. Microinjection reagents

A translation-blocking antisense morpholino, targeting *X. tropicalis katnal2* (Table S1), was injected at a range between 1 pmol to 6 pmol, with *X. tropicalis* blastomeres receiving 2 nl and *X. laevis* 10 nl. Mouse *KATNAL2-GFP* (Ververis et al., 2016) was subcloned into *pCS108* and *in vitro* transcribed using *Not*I restriction enzyme and the mMessage SP6 polymerase kit (Thermo Fisher Scientific). One blastomere at the two-cell stage was injected with 300 pg of *in vitro* transcribed mRNA. *Centrin4-CFP/Centrin4-RFP* (Antoniades et al., 2014; Park et al., 2008) was *in vitro* transcribed using *Asc*I restriction enzyme and the mMessage SP6 polymerase kit (Thermo Fisher Scientific); 300 pg of mRNA was co-injected with 300 pg *KATNAL2-GFP mRNA*. The negative control for morpholino injection was an injection of 300 pg of *Centrin4-CFP* mRNA alone.

2.9. CRISPR-based genome editing

Two methods were used for single guide RNA (sgRNA) synthesis. First, two non-overlapping sgRNAs targeting *katnal2* and 1 control sgRNA targeting the pigmentation gene *slc45a2* were designed by CRISPRscan (Moreno-Mateos et al., 2015) using *X. tropicalis* genome version 9.0 (see Table S1 for target and oligonucleotide sequences). Oligonucleotides were synthesized by Elimbio, and sgRNAs were *in vitro* transcribed (NEB Engen sgRNA synthesis kit) and purified (Zymo Clean and Concentrator column). sgRNAs were combined with Cas9-NLS protein (MacroLabs, UC Berkeley), and an Alexa-555-labeled dextran (Thermo Fisher). *X. tropicalis* embryos were injected into one cell at the two-cell stage with 3 ng Cas9 and 800 pg sgRNA.

The second method for sgRNA synthesis used the IDT Alt-R™ system (Integrated DNA Technologies; USA). The same target sequences were used as above with the addition of a scrambled CRISPR#1 sgRNA sequence as negative control (Table S1). Ribonucleoproteins (RNPs) were assembled with Alt-R™ tracrRNA (IDT #146107918) and recombinant Cas9-NLS protein (MacroLabs, UC Berkeley) according to IDT instructions. One cell of two-cell stage *X. tropicalis* embryos was injected with 1.5 ng Cas9 and 400 pg sgRNA.

For *in vitro* testing of the sgRNAs, IDT RNPs were assembled as above and incubated for 30 min at 37 °C with 200–400 ng of a full-length *katnal2* PCR amplicon in duplex buffer (100 mM Potassium Acetate, 30 mM HEPES, pH 7.5). Products were purified (Zymo DNA clean and concentrator kit), and the activity of the RNP on the synthetic template was evaluated by DNA electrophoresis (Fig. S4B, C).

2.10. Genotyping

X. tropicalis embryos were genotyped by Fragment Length Analysis (FLA) (Bhattacharya et al., 2015). Briefly, individual embryos were collected and snap frozen in liquid nitrogen. Genomic DNA was extracted and subjected to two rounds of PCR. The first PCR reaction consisted of 25 cycles with 100 ng genomic DNA, amplified with primers flanking the editing site (Table S1) at 0.5 μM each and HiFi polymerase HotStart MM (NEB) in a total volume of 15 μl. Forward primers harbored an additional 5' FamF sequence extension of AGCTGACCGGCAGCAAAATTG (Yang et al., 2015). The second PCR reaction (15 cycles) was set up with further addition of 1 μl of 10 μM fluorescently-tagged primer to the FamF extension (6-FAM; Table S1), 1 μl of 10 μM reverse primer (as per the first PCR round in each case) and 2 μl of HiFi polymerase HotStart MM (NEB). Upon completion of the second round of PCR, an aliquot of 0.5 μl PCR product with 11 μl of Hi-Di formamide and the addition of LIZ500 size standards was subjected to FLA by the UC Berkeley DNA Sequencing Facility. The CRISPR#1 locus appeared to have a wild-type allele polymorphism: approximately half of the products in control embryos were 361 basepairs (bp) and the other half were 365 bp in length. Apparent heterozygotes have both peaks. Fig. S4D represents a 365 bp example.

2.11. Microscopy and Image Processing

Whole mount immunofluorescence images were acquired with 25 ×, 40 ×, and 63X objectives on a Zeiss LSM710 or a Leica SP8 confocal microscope. Tadpole heads were imaged using an Apotome setup with a 1X objective on a Zeiss AxioZoom V16 microscope. Cell immunofluorescence images were acquired with a Zeiss Apochromat 639 NA 1.4 oil lens on a Zeiss Axiovert 200 M inverted microscope, equipped with an AxioCamMRm camera. RNA *in situ* hybridization and gross phenotypes were imaged on a Zeiss AxioZoom V16 microscope. Images were compiled with ImageJ (Fiji, NIH). Some images were processed in Abobe Photoshop CC, and all images were assembled into figures in Adobe Illustrator CC.

2.12. Telencephalon and ventricle size quantification and analysis

Telencephalon and 1st ventricle size was measured manually in ImageJ (Fiji, NIH) using the freehand selection tool and the area measure function from images like those in Fig. 7A and D, acquired with a 1X objective on a Zeiss AxioZoom V16 microscope. For the telencephalon, measured area included the entire olfactory bulb and pallium, but did not include the more posterior diencephalon. For the 1st ventricle, measurements included the 1st ventricle area up to the midline, but excluded the diencephalon. Injected and uninjected area measurements were made from the same images and compared by a two-tailed Wilcoxon matched-pairs signed rank sum test for statistical significance.

3. Results

3.1. katnal2 isoforms are maternally expressed and enriched in ciliated tissues and the developing nervous system

To initiate the analysis of *katnal2* gene expression, we designed PCR primers at the extremities of the 16-exon locus encoding *katnal2* in *Xenopus tropicalis,* and we identified by RT-RCR and sequencing two alternatively spliced isoforms, consistent with the existence of multiple isoforms in mouse and human (Fig. S1A-B). The two *X. tropicalis* isoforms displayed the typical protein sequence elements of katanin (AAA, MT-binding and Walker motif signature sequences), the shorter one lacking a 32 amino acid sequence encoded by exon 6 (Fig. S1B, grey shading). Both isoforms harbored the LisH motif, a sequence important in self-association, MT-binding or protein-protein interactions with ATPases (Emes and Ponting, 2001), which is also found in the longer isoforms in mice (Ververis et al., 2016). Subsequent semi-quantitative RT-PCR analysis of *katnal2* expression during embryonic *X. tropicalis* development revealed that both *katnal2* isoforms were maternally inherited as well as expressed by the embryo after the onset of zygotic transcription at stage 9 (Fig. S1C). During the stages sampled, the relative stoichiometry between the two isoforms did not show major fluctuation, with the longer isoform being expressed more prominently throughout (Fig. S1C). In agreement with the RT-PCR, whole mount RNA *in situ* hybridization in *X. tropicalis* revealed maternal *katnal2* mRNA in early embryos (Fig. S1D-G). At gastrula-

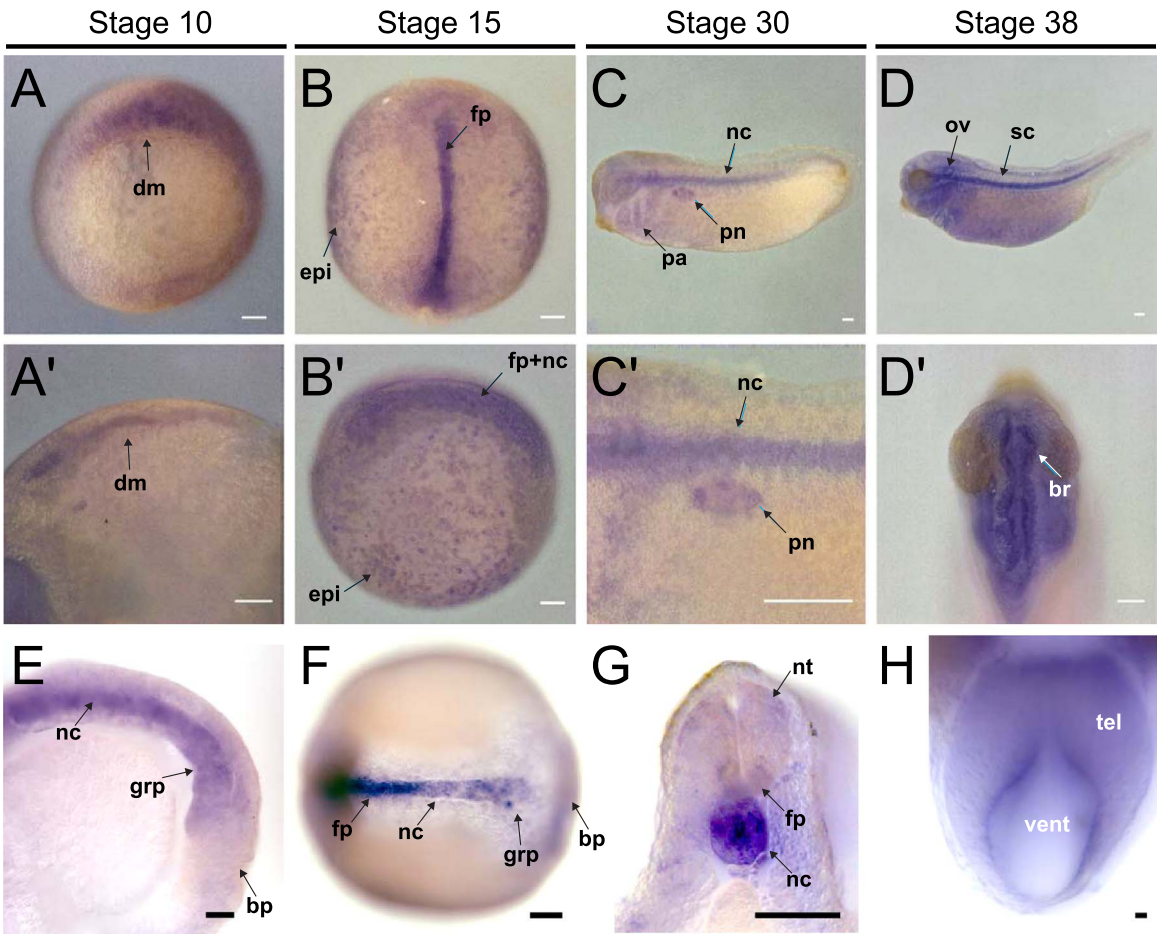

Fig. 1. *katnal2* is expressed in ciliated tissues and the developing nervous system. A-H) Whole mount RNA *in situ* hybridization for *katnal2* during *X. tropicalis* development. A) *katnal2* expression is enriched in the dorsal mesoderm (dm). A') Transverse section of A. B) Dorsal view of *katnal2* expression in the floor plate (fp) and epidermis (epi). B') Lateral view of B, anterior to the left also showing notochord (nc) staining. C) Lateral view of *katnal2* expression enriched in the nc, pronephric nephrostomes (pn), and pharyngeal arches (pa). C') Higher magnification view of C highlighting pn and nc expression. D) Lateral view of *katnal2* expression in the spinal cord (sc) and otic vesicle (ov). D') Dorsal view of *katnal2* expression in the brain (br), especially in the cells lining the ventricles. E) Sagittal section of stage 15 embryo showing expression in the gastrocoel roof plate (grp), anterior to the blastopore (bp). F) Coronal section showing an interior dorsal view of a stage 15 embryo, with expression in the nc and grp. G) Transverse section of a stage 30 embryo showing expression in the neural tube (nt), floor plate (fp), and notochord (nc). H) Coronal section of stage 38 embryo showing high expression in the cells lining the telencephalic (tel) ventricle (vent). Abbreviations: dm = dorsal mesoderm; fp = floor plate; epi = epidermis; nc = notochord; pn = pronephric nephrostomes; pa = pharyngeal arches; ov = otic vesicle; sc = spinal cord, br = brain; grp = gastrocoel roof plate; bp = blastopore; nt = neural tube; vent = ventricle; tel = telencephalon. Scale: 100 μm, except H where Scale: 10 μm.

tion, *katnal2* was present at the dorsal lip of the blastopore, including the dorsal mesoderm (Fig. 1A,A'). During neurulation, strong *katnal2* expression was observed in the notochord (Fig. 1B,B',E-F), and relatively low expression was detected in the neural floor plate. Expression was also observed in the epidermis (Fig. 1B,B'), as well as in the gastrocoel roof plate (GRP). By tailbud stages (stage 30 and later), expression was most prominent in the notochord and the brain, and additional staining was observed in the developing nephrostomes, otic vesicles, and pharyngeal arches (Fig. 1C-D,G). In the developing brain, *katnal2* expression was strong in the cells lining the ventricles (Fig. 1D',H). Taken together, *katnal2* was predominantly expressed in the developing nervous system and in highly ciliated tissues, such as the dorsal mesoderm, floor plate, GRP, epidermis, nephrostomes, otic vesicles, and brain ventricles.

3.2. Katnal2 localizes to cilia, basal bodies, centrioles, and mitotic spindles

To reveal the subcellular localization of Katnal2 protein *in vivo*, we used two different antibodies raised against the murine KATNAL2 protein and overexpressed GFP-tagged murine KATNAL2 in *Xenopus* embryos. In multiciliated cells of the *X. tropicalis* embryonic epidermis, Katnal2 localized along ciliary axonemes (Fig. 2A), and at higher magnification, Katnal2 appeared in a dense punctate pattern (Fig. 2B; which was specific to the Katnal2 antibody Fig. S2). Furthermore, Katnal2 was also localized at the basal bodies in multiciliated cells (Fig. 2C,E), at the centrioles of non-ciliated cells (Fig. 2F-G), and at the midbodies of dividing cells (Fig. 2F,H). Correspondingly, we observed localization of Katnal2 at centrioles, the mitotic spindle, basal bodies and primary cilia in the *X. laevis* cell line XL177 (Fig. S3). In stage 45 tadpoles, Katnal2 was expressed broadly, but enriched in highly ciliated cells, such as those lining the first ventricle of the brain (Fig. 3B), those lining the olfactory epidermis (Fig. 3C), those in the eye (Fig. 3D), those at the roof of the fourth ventricle (Fig. 3E), and in the pronephric kidney (Fig. 3F). Staining was also prominent on the spindle of cells undergoing mitosis in the developing brain (Fig. 3B',B"). Co-localization with a poly-glutamylation antibody confirmed axonemal puncta along ciliary axonemes of the cells lining the olfactory epithelium (Fig. 3C). Taken together, the mRNA expression patterns and protein localization data in *Xenopus* embryos collectively suggested a possible functional role for Katnal2 in ciliation and nervous system development.

3.3. katnal2 is required for Xenopus embryonic development

In order to assess the impact of Katnal2 loss-of-function on embryonic development, we generated translation-blocking antisense

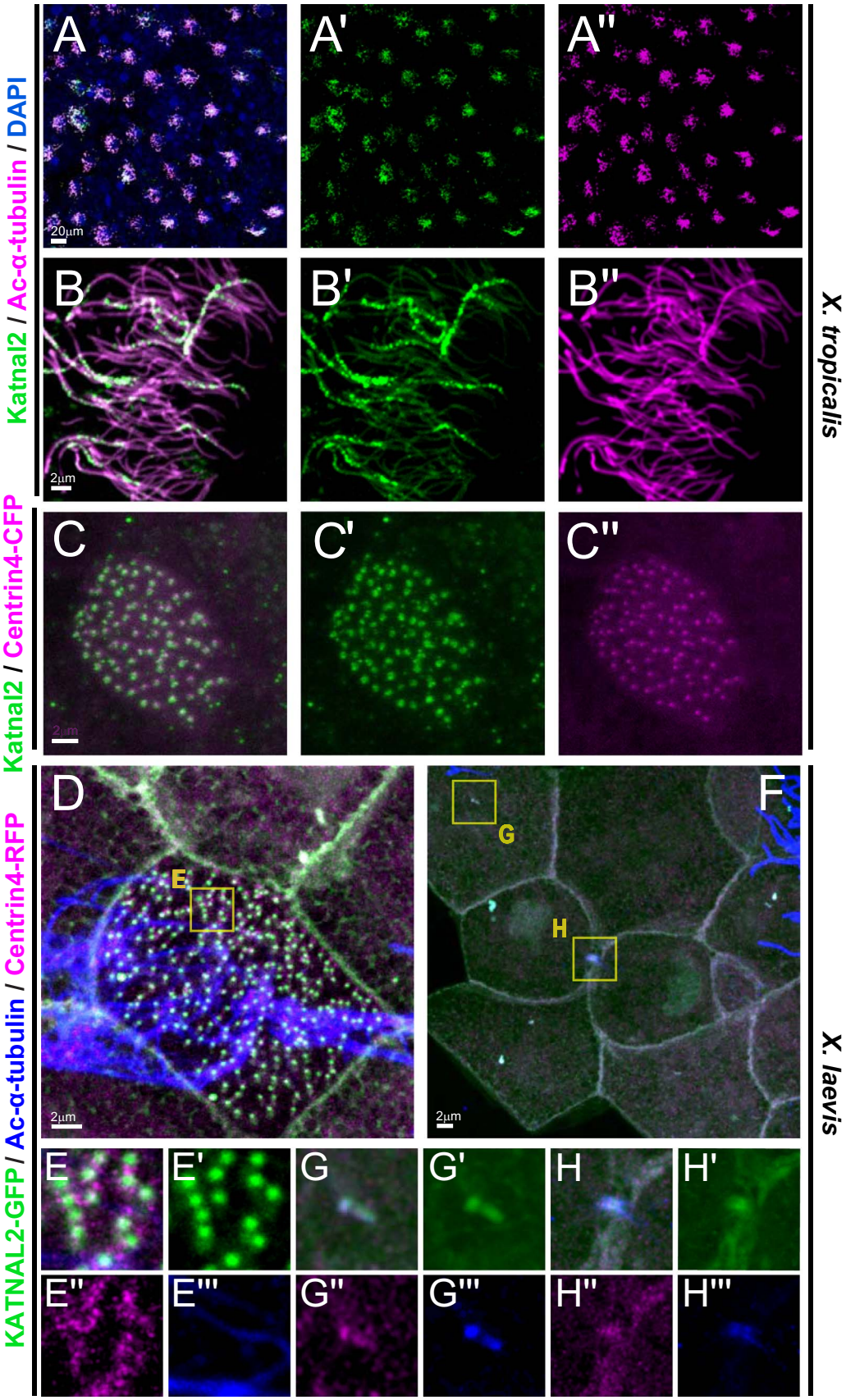

Fig. 2. Katnal2 localizes to epidermal cilia, basal bodies, and centrioles. A-B) Katnal2 rabbit antibody staining (green) of *X. tropicalis* multiciliated cells of the epidermis, co-stained with DAPI (nuclei, blue) and acetylated α-tubulin (Ac-α-tubulin; cilia, magenta). B) High-magnification image from the specimen shown in A. C) Katnal2 antibody staining (green) with Centrin4-CFP expression (magenta). D-H) KATNAL2-GFP (green) in the embryonic epidermis of *X. laevis*, co-stained for Centrin4-RFP (basal bodies/centrioles, magenta) and Ac-α-tubulin (cilia, blue). D-E) KATNAL2-GFP localizes to basal bodies in multiciliated cells. (E is close-up of D) F-H) KATNAL2-GFP localization in non-ciliated epidermal cells. G) KATNAL2-GFP signal in centrioles. H) KATNAL2-GFP signal in the midbody of dividing cells.

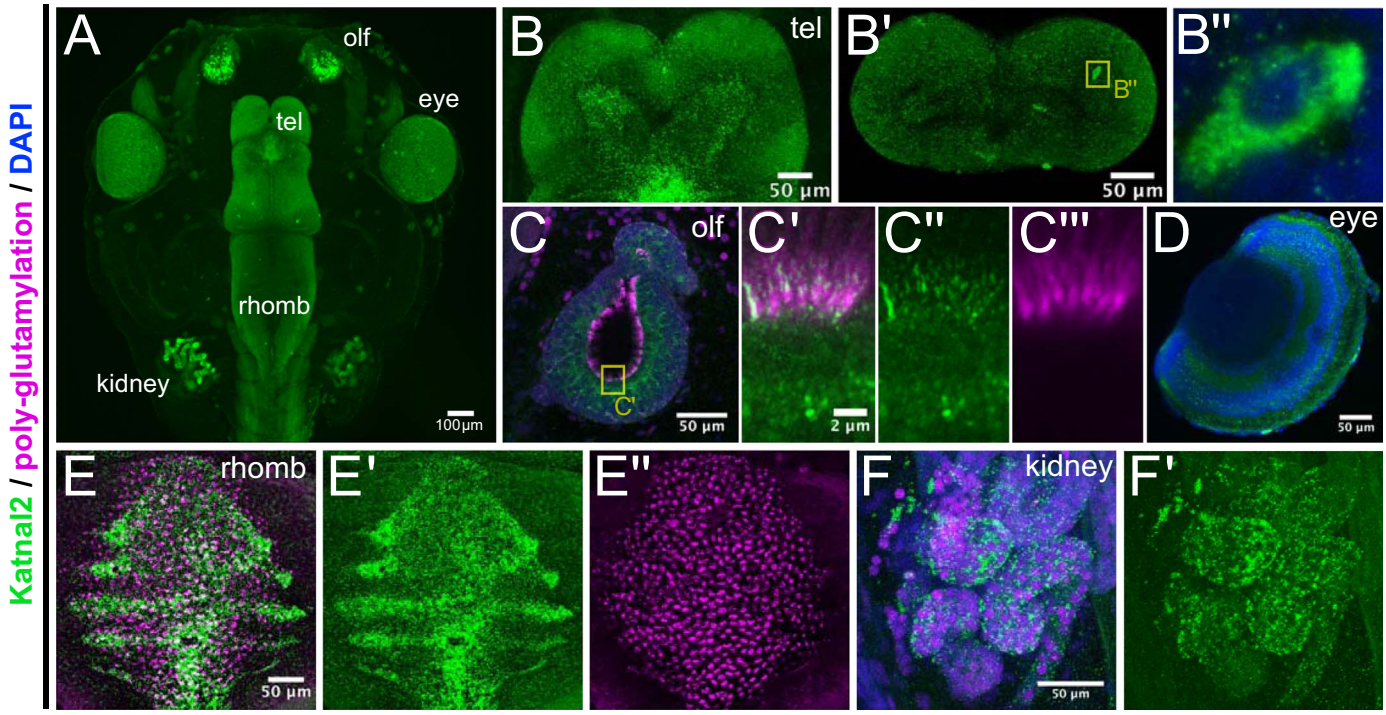

Fig. 3. Katnal2 localizes to mitotic spindles and ciliary axonemes in the tadpole. A-F) Katnal2 rabbit antibody staining (green) in stage 45 *X. tropicalis* tadpoles, highlighting staining in ciliated and neural tissues. A) Low magnification view of Katnal2 staining in the cephalic region of the tadpole. B) Telencephalic (tel) region of the brain, showing expression throughout and especially within the first ventricle. B') Transverse section through the telencephalon. B") High-magnification image from specimen shown in B', showing Katnal2 localization to a mitotic spindle. C) Olfactory epithelium (olf) stained for Katnal2 (green), poly-glutamylation (cilia, magenta) and DAPI (nuclei, blue). C'-C"') High-magnification image of the specimen in C, showing localization of Katnal2 (green) to ciliary axonemes (poly-glutamylation, magenta). D) Eye. E) Multiciliated cells of the roof of the fourth ventricle of the rhombencephalon (rhomb). F) Katnal2 is expressed throughout the kidney. Abbreviations: tel = telecephalon; olf = olfactory epithelium; rhomb = rhombencephalon.

morpholino oligonucleotides and two non-overlapping sgRNAs synthesized by two different methods (*in vitro* transcription or IDT Alt-R synthesis). We also generated a scrambled sgRNA as negative control and a sgRNA against the pigmentation gene *slc45a2* as positive control. We used an *in vitro* assay to confirm efficient and correct targeting of *X. tropicalis katnal2* cDNA by *katnal2* sgRNA/Cas9 RNPs, but not by the scrambled sgRNA/Cas9 RNP (Fig. S4A-C). Next, *X. tropicalis* embryos were injected with sgRNA RNPs, and genotyping of individual embryos by Fragment Length Analysis demonstrated efficient *in vivo* gene targeting by both sgRNAs against *katnal2* (Fig. S4D).

katnal2 knockdown by translation-blocking antisense morpholino oligonucleotides or mutation by CRISPR/Cas9-mediated genome editing both led to defects in convergent extension, including blastopore and neural tube closure defects (Fig. 4A, B), and shortened length of the anterior-posterior axis (Fig. 4C). These phenotypes were reminiscent of phenotypes observed following loss of Katnal2 interactor protein Nubp1 in *Xenopus* (Ioannou et al., 2013). In later developmental stages, loss of *katnal2* caused further defects in anterior-posterior axis elongation, cranial cartilage development, melanocyte migration, and eye pigmentation, with morpholino knockdown acting in a dose-dependent manner and having an overall stronger effect than CRISPR/Cas9 genome editing (Fig. 5A-D, S4F). These results further confirmed the specificity of manipulations, and differences in efficiency were likely a result of MOs targeting maternal and zygotic transcripts, while CRISPR/Cas9 treatment only affected zygotically derived gene expression. Specifically, following loss of *katnal2*, eye size and eye pigmentation were reduced (Fig. 5A-D, S4F), melanocytes were not properly localized (Fig. 5C, S4F), and cranial cartilage was dramatically reduced (Fig. 5A-D), suggesting defects in neural crest specification or migration. To specifically determine whether these phenotypes arose from defects in the specification or migration of neural crest cells, we assayed expression of *snail2* by RNA *in situ* hybridization following *katnal2* loss-of-function. In all manipulations, *snail2*-expressing cells were detected, but showed defects in migration (Fig. 5E), consistent with a role for Katnal2 in cell polarity affecting neural crest cell migration. Additionally, embryos often showed edema, indicating kidney malfunction (data not shown). We also observed similar phenotypes using MO-mediated knockdown in *X. laevis* (Fig. S5A-B). In contrast, scrambled sgRNA-injected animals were comparable to controls concerning all of the above aspects while *slc45a2* sgRNA-injected animals displayed the expected loss of eye and body pigmentation specifically on the injected side (Fig. S4E), but no other phenotypes were observed.

Taken together, these experiments revealed a requirement for *katnal2* during embryonic development and organogenesis in *X. tropicalis* and *X. laevis* embryos by two independent loss-of-function approaches. Furthermore, while we expect morpholino oligonucleotides to target maternal stores of mRNA, the sgRNA/Cas9 RNP will only target zygotic expression. Thus, it is not surprising that the manipulations permit mitosis and survival of cells early on, but have their greatest effects on those tissues that require higher levels of zygotic expression of *katnal2* for ciliation or very active proliferation.

3.4. *katnal2* is required for ciliogenesis and brain development

Given the localization of Katnal2 at basal bodies and in axonemes, we next specifically investigated cilia formation in multiciliated cells of the embryonic epidermis (Brooks and Wallingford, 2014; Walentek and Quigley, 2017). After morpholino knockdown or CRISPR-mediated mutagenesis of *katnal2*, we observed ciliogenesis defects. Specifically, targeted multiciliated cells showed reduced ciliation, and the remaining cilia appeared shorter than in non-targeted multiciliated cells in both *X. tropicalis* (Fig. 6A-J) and *X. laevis* (Fig. S5C-E). These phenotypes scaled in a dose-dependent manner and were accompanied by defects in basal body distribution and apical actin network formation (Fig. S6A-C).

Given the pronounced localization of Katnal2 in the developing nervous system, we next assayed the effects of *katnal2* loss-of-function

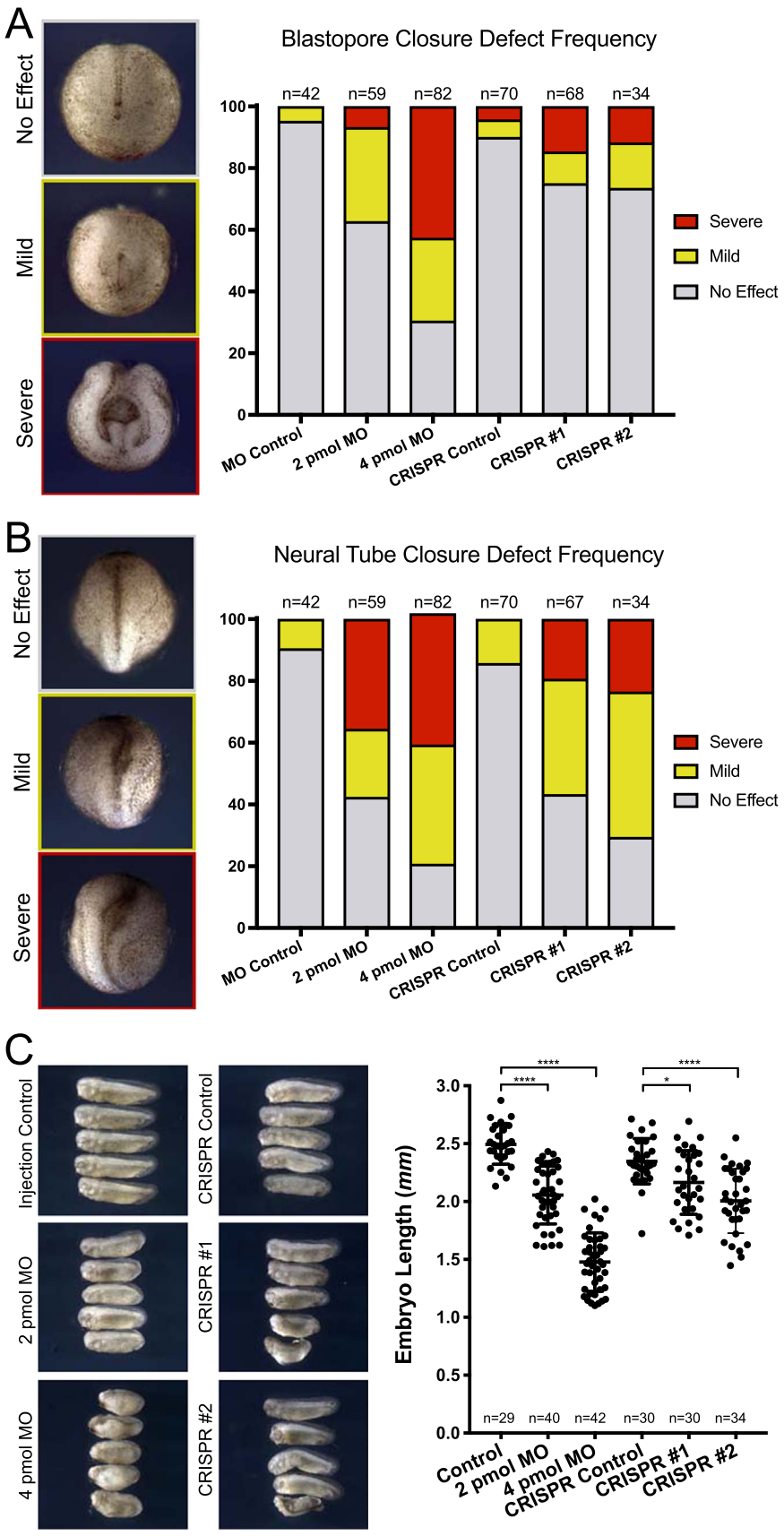

Fig. 4. *katnal2* is required for blastopore closure, neural tube closure, and anterior-posterior axis elongation in *X. tropicalis*. A) *katnal2* inhibition leads to incomplete blastopore closure. Shown are representative phenotypes (no effect, mild, and severe) with quantification by condition. MO control is injection of *Centrin4-CFP* mRNA. CRISPR control is targeting of *slc45a2*. B) *katnal2* inhibition leads to defects in neural tube closure. Shown are representative phenotypes (no effect, mild, and severe) with quantification by condition. MO control is injection of *Centrin4-CFP* mRNA. CRISPR control is targeting of *slc45a2*. C) *katnal2* inhibition leads to shortened anterior-posterior axis elongation. Embryo length from head to tail was measured and plotted by condition. MO control is injection of *Centrin4-CFP* mRNA. CRISPR control is targeting of *slc45a2*. *: $p < 0.05$; ****: $p < 0.001$.

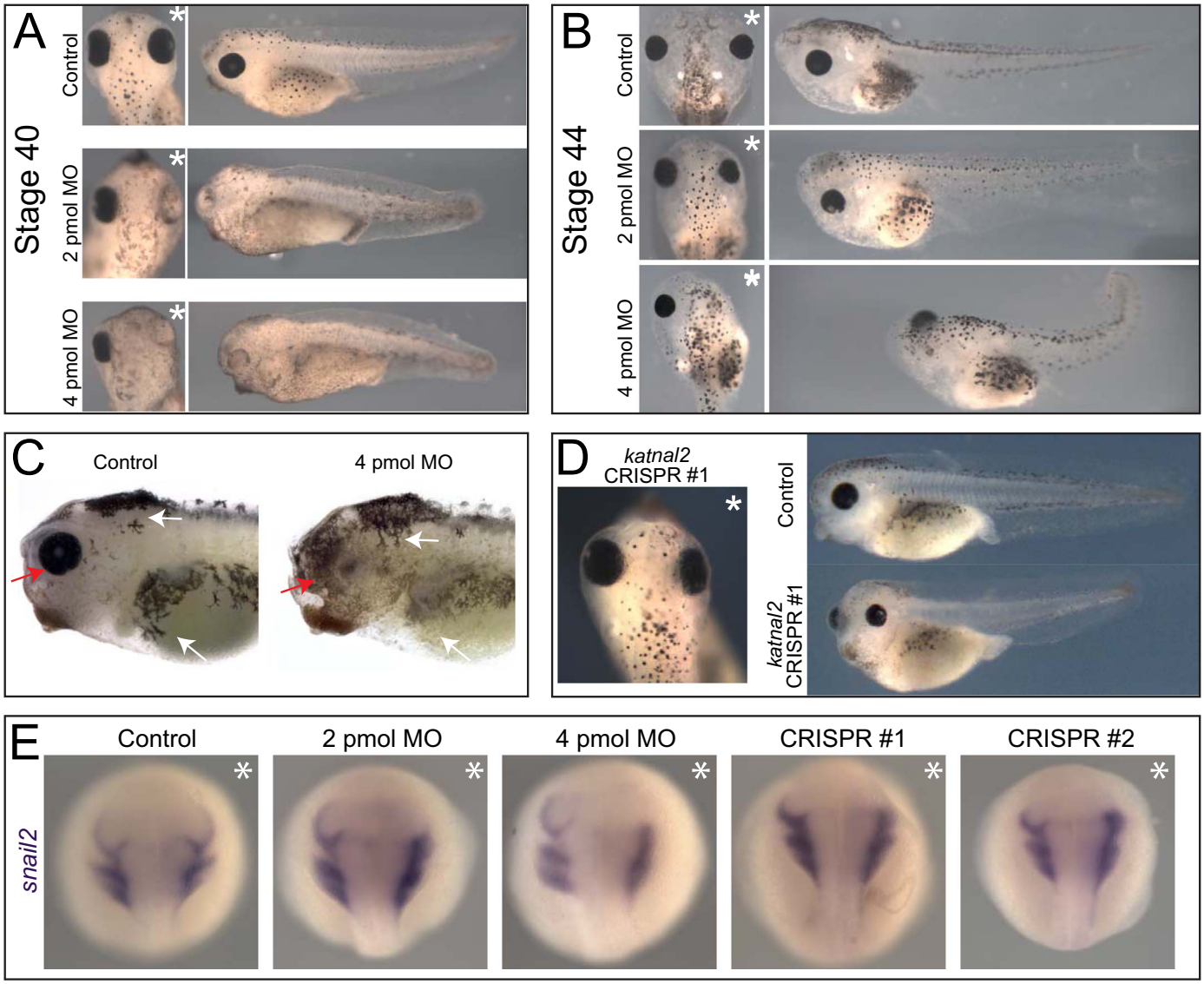

Fig. 5. *katnal2* is required for eye, pigmentation, and neural crest development in *X. tropicalis*. A) Representative embryos at stage 40 following injection of a *katnal2* translation-blocking morpholino into half of the embryo. Morpholino dose indicated on the left. Asterisk (*) indicates injected side of the embryo. The injected side shows defects in axis elongation, eye formation, cranial cartilage development, and pigmentation. Control embryos were injected with *Centrin4-CFP* mRNA. B) Representative embryos at stage 44 following injection of *katnal2* morpholino. Asterisk (*) indicates injected side of the embryo. Injected animals show defects in axis elongation, eye formation, and cranial cartilage formation. Control embryos were injected with *Centrin4-CFP* mRNA. C) *katnal2* morpholino-injected animals show defects in pigmentation (white arrows), especially migration of melanocytes, and defects in eye formation (red arrow). Control embryos were injected with *Centrin4-CFP* mRNA. D) Representative embryos at stage 44 following genome targeting of *katnal2* by CRISPR/Cas9 into half of the embryo. Asterisk (*) indicates injected side. *katnal2*-targeted embryos show defects in eye formation, cranial cartilage formation, and pigmentation on the injected side. Control embryos were injected with Cas9 protein and a scrambled sgRNA. E) Stage 18 embryos following RNA *in situ* hybridization against *snail2*, labeling neural crest. Asterisk (*) indicates injected side. *katnal2* loss-of-function inhibits neural crest migration. Control embryos were injected with *Centrin4-CFP* mRNA.

during embryonic brain development. Since human mutations in *KATNAL2* associated with neurodevelopmental disorders are heterozygous (Iossifov et al., 2014; Neale et al., 2012; O'Roak et al., 2012; Sanders et al., 2012; Stessman et al., 2017; Willsey et al., 2013), we investigated the more attenuated phenotypes by low-dose *katnal2* MO injections. Strikingly, this *katnal2* knockdown resulted in reduced brain size, particularly in the telencephalic region (Fig. 7A-C; size 29,397 ± 3472 μm^2 in controls *vs*. 22,248 ± 3594 μm^2 in morphants; $p < 0.0001$; $n = 37$). To further investigate this observation, and given the role of Katnal2 in cell division (Ververis et al., 2016), we next assayed whether there were accompanying changes in the number of ventricular zone progenitor cells in morphants, using proliferative cell nuclear antigen (PCNA) antibody staining (Fig. 7D-G). Quantification confirmed that the injected side displayed a smaller proliferative area around the first ventricle (10,415 ± 2022 μm^2 in controls *vs*. 7902 ± 1911 μm^2 in morphants; $p < 0.0001$; $n = 25$). Taken together, our *in vivo* functional studies confirmed the requirement for Katnal2 in cilia formation and further revealed an important role for Katnal2 during brain development.

4. Discussion

Here we show the expression and localization of Katnal2 during *Xenopus* development, and characterize its essential roles in ciliogenesis and organogenesis, including brain development. *katnal2* expression is highly enriched in the developing *Xenopus* epidermis, kidney, brain, eye, and inner ear, all tissues known to be highly ciliated (Schweickert and Feistel, 2015; Walentek and Quigley, 2017). Katnal2 protein is localized to basal bodies, ciliary axonemes, centrioles, and mitotic spindles in several developing tissues. Consistently, *katnal2* loss-of-function induces deficits in ciliogenesis, including aberrant basal body behavior, apical actin formation and ciliogenesis.

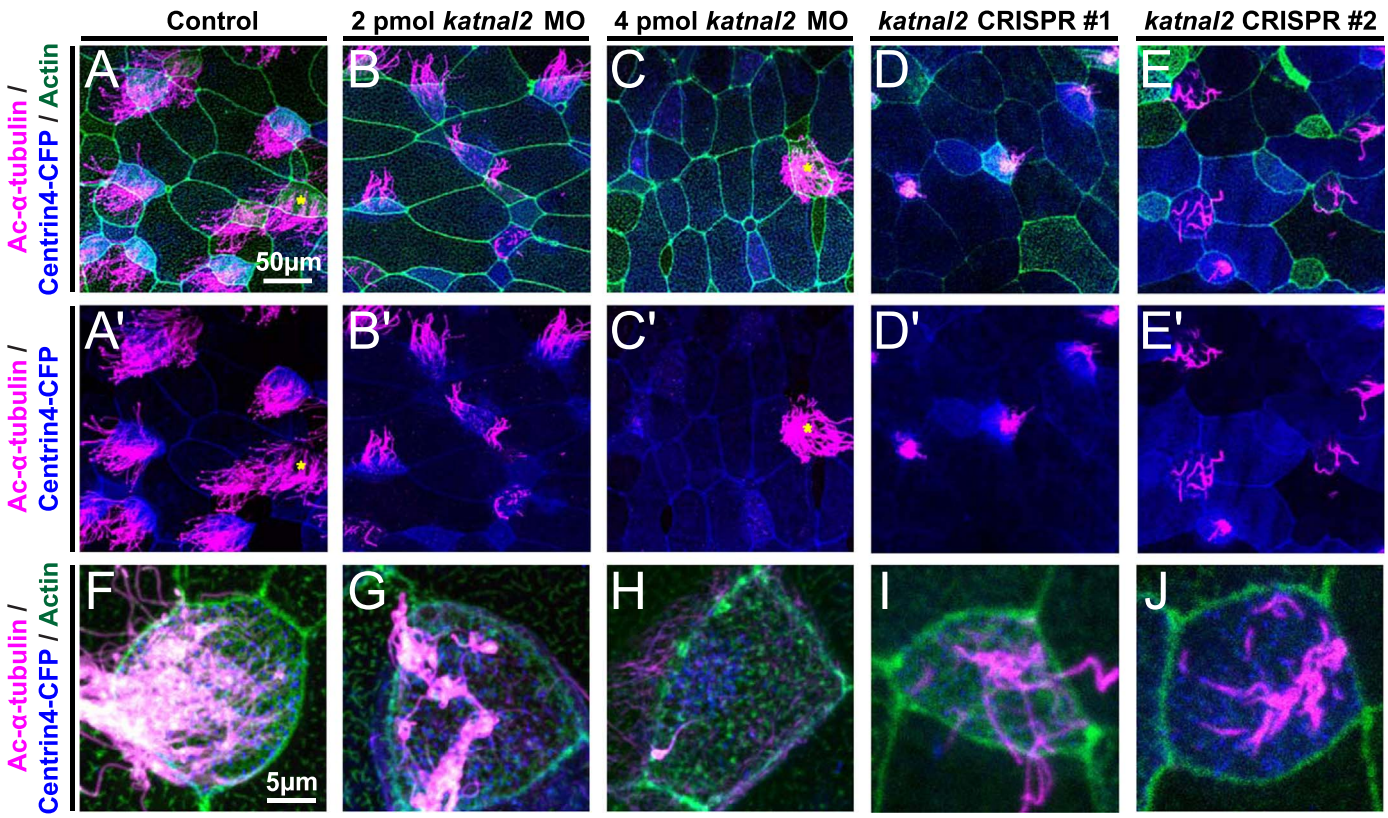

Fig. 6. *katnal2* is required for ciliogenesis. A-J) Multiciliated *X. tropicalis* embryonic epidermis following injection of *katnal2* morpholino at two doses or CRISPR/Cas9 RNP, showing Centrin4-CFP (blue), Actin (phalloidin, green) and acetylated α-tubulin (Ac-α-tubulin, cilia, magenta). A) Control embryos (injected with Centrin4-CFP alone) show normal ciliogenesis. B-C) Embryos injected with 2–4 pmol of *katnal2* morpholino show reduced number and length of cilia. D-E) Embryos injected with *katnal2* CRISPR/Cas9 RNPs also show reduced number and length of cilia. F-J) High magnification view of each condition. Asterisks (*) mark cells that did not undergo *katnal2* disruption (Centrin4-CFP negative).

The punctate localization of Katnal2 in ciliary axonemes suggests dynamic regulation of microtubules during axoneme formation and maintenance. Although Katnal2 severing activity on MTs has not been formally demonstrated or measured in *Xenopus* or other species using typical *in vitro* assays with purified MTs, its localization and silencing phenotypes in both mouse and *Xenopus* strongly suggest such a function. Katnal2's similarities in sequence, localization, and function with archetypal Katanin, whose MT-severing molecular mechanism has been deciphered (Hartman and Vale, 1999), further strengthens the hypothesis that Katnal2 likely has the ability to remodel MTs at different cellular locations (ciliary axoneme, spindle, MT network) and cell cycle phases (interphase and mitosis). Nevertheless, Katnal2's MT-severing activity will need to be specifically characterized in the future.

The ciliogenesis defects observed after loss of *katnal2* in this work closely mirror the ciliary phenotypes in *X. laevis* morphants for *nubp1*, a Katnal2-interacting protein (Ioannou et al., 2013). The sustained and widely overlapping expression of *nubp1* and *katnal2*, together with similar loss-of-function phenotypes in ciliogenesis are consistent with their implicated physical and functional interactions in *Xenopus*, similar to those described in the mouse (Ververis et al., 2016). Furthermore, *nubp1* knockdown also induces defects in blastopore and neural tube closure, and results in the shortening of the anterior-posterior axis, like *katnal2* deficiency. These results suggest that Nubp1 and Katnal2 may function together during convergent extension and ciliogenesis in *Xenopus* development. Additionally, our results also show that Katnal2 is essential for normal vertebrate organogenesis, playing key roles in neural crest migration, eye formation, pigmentation, and kidney development.

The observed effects after Katnal2 loss-of-function on blastopore and neural tube closure as well as neural crest cell migration and organization of apical actin in multiciliated cells suggest a role for Katnal2 during the regulation of Wnt/planar cell polarity (PCP)-dependent processes. Similar effects were previously described after manipulation of other ciliary components (Wallingford and Mitchell, 2011), but it is still not fully resolved whether those effects are primarily caused by loss of cilia or through the involvement of ciliary and centriolar proteins in the establishment of cellular polarity directly. Interestingly, it was demonstrated that subapical microtubules are required for sorting of core PCP components into stable complexes during the establishment of PCP (Matis et al., 2014; Walentek and Quigley, 2017). Thus, Katnal2's MT severing function could contribute to the formation, organization or maintenance of subapical MTs required for stable PCP complex formation. Such a possibility should be addressed in future experiments to further investigate a potential connection between Wnt/PCP and MT-severing protein function.

Recently, human *KATNAL2* was identified as a high-confidence risk gene for autism spectrum disorders (ASD) (Iossifov et al., 2014; Neale et al., 2012; O'Roak et al., 2012; Sanders et al., 2012; Stessman et al., 2017; Willsey et al., 2013). Therefore, it is interesting to note that loss of *katnal2* leads to reduced telencephalon size. Furthermore, *katnal2* was highly expressed in the proliferative cells lining embryonic *Xenopus* brain ventricles, and human *KATNAL2* expression appears to be specific to ventricular zone cells sequenced from 15 weeks post-conception human cortex (Parikshak et al., 2013). The role of Katnal2 in brain size control could reflect a role for Katnal2 in polarity and directional cell division, especially given its localization in centrioles and mitotic spindles of telencephalic progenitors (Fig. 3B'-B"). Alternatively Katnal2 could influence proliferation through indirect effects *via* ciliary signaling (Guo et al., 2015). Likewise, potential roles for Katnal2 in post-mitotic processes during *Xenopus* brain development (*e.g.* axon outgrowth and migration of differentiating neurons) are plausible and will be addressed in the future. Importantly, it will be

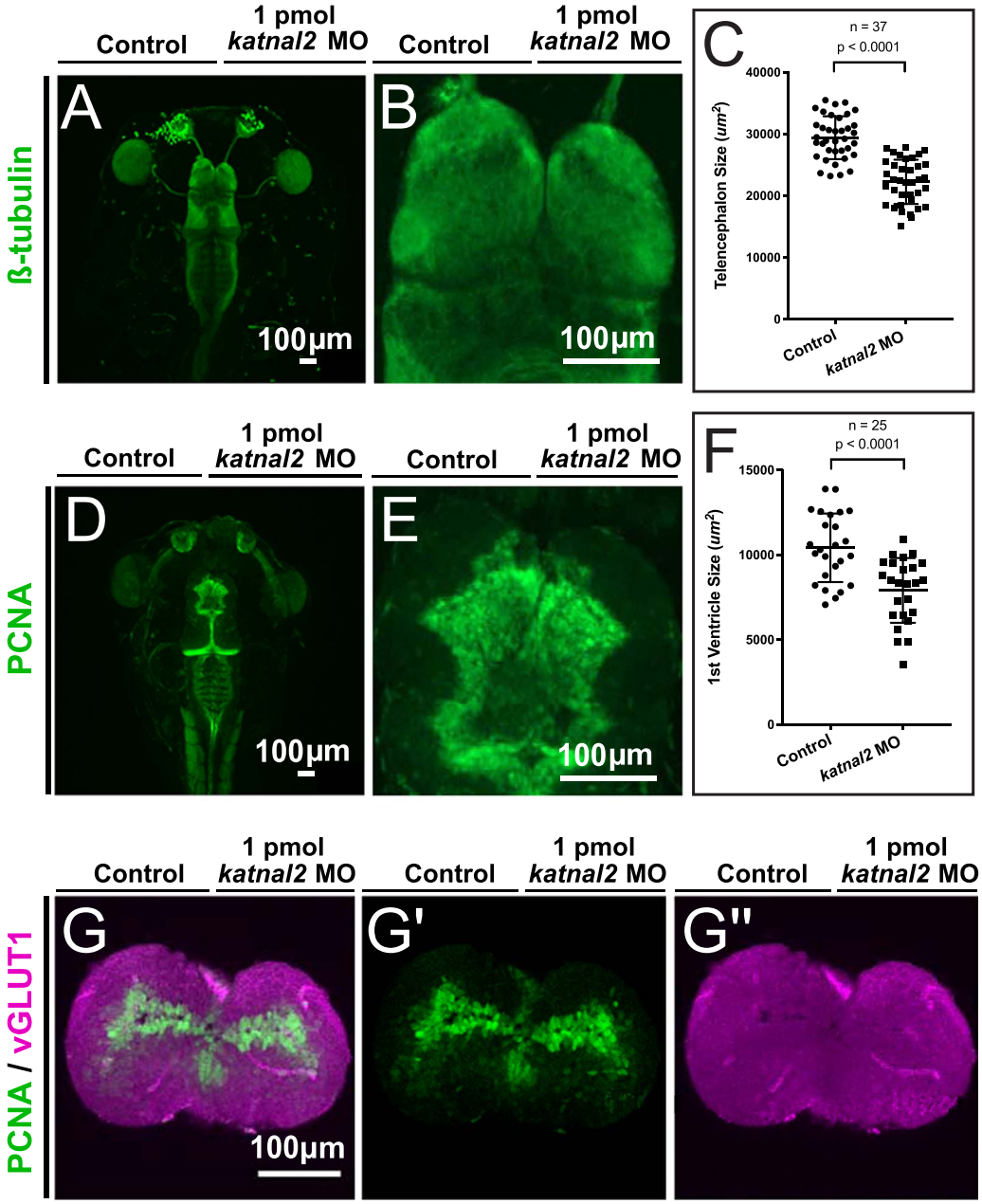

Fig. 7. *katnal2* is required for telencephalon development in *X. tropicalis*. A) Representative stage 46 *X. tropicalis* tadpole, following 1 pmol *katnal2* morpholino injection into half of the embryo, stained for β-tubulin to visualize the nervous system. B) Close-up of the telencephalic region in A. C) Quantification of telencephalon size, comparing the uninjected side of the tadpole to the injected side, reveals reduced size on the morpholino-injected side ($p < 0.0001$; $n = 37$). D) Representative stage 46 *X. tropicalis* tadpole following 1 pmol *katnal2* morpholino injection into half of the embryo, stained for proliferating cell nuclear antigen (PCNA) to visualize the proliferative cells of the nervous system, shows a reduction of area on the morpholino injected side. E) Close up of the telencephalic region (first ventricle) from D. F) Quantification of PCNA positive area in the telencephalic region (first ventricle), comparing the uninjected side to the injected side ($p < 0.0001$; $n = 25$). G) Transverse section of telencephalic region, stained for PCNA (ventricular zone progenitors, green) and vGLUT1 (glutamatergic neurons, magenta).

essential to address in future studies which of these effects are primary to the loss of Katnal2 or secondary to the change of overall telencephalic cell numbers, cilia formation or cell polarity. This is especially critical since KATNAL2 was found important for proper dendritic arborization in mouse embryonic dentate gyrus developing neurons (Williams et al., 2016). Intriguingly, Spastin (SPAST), a microtubule-severing protein similar to KATNAL2 (Eckert et al., 2012), is also an ASD risk gene (Sanders et al., 2015), suggesting its potential in similar processes to those described here.

Finally, this work highlights the power of *Xenopus tropicalis* for cost-effective analysis of neurodevelopmental disorder risk gene function in a developing diploid vertebrate. Injection of CRISPR-Cas9 RNPs into one cell of two-cell stage embryos allows for direct comparison of neurodevelopmental phenotypes within a living organism and circumvents the need for time-intensive breeding strategies.

Acknowledgements

We thank Matthew State for generous and steadfast support. We thank Jeremy Willsey and Paris Skourides for critical reading of the manuscript. We are grateful to Romain Gibeaux and Kelly Miller (Heald laboratory) for expert technical advice; Edivinia Pangilinan (Harland laboratory) for expert technical help; Giannis Maimaris (Santama laboratory) for assistance with XL177 immunofluorescence; Gary Moulder, Kelly Jensen, Nolan Wong, and Shaun Coughlin for support at the UCSF *Xenopus* facility; James Evans for support at the UC Berkeley *Xenopus* facility.

Author contributions

Project conception: NS
Experimental planning: HRW, PW, NS
Performed experiments: HRW, PW, CRTE, YX, ABL, NS
Interpretation of results: HRW, PW, NS
Wrote manuscript: HRW, PW, NS
Edited manuscript: all authors

Competing interests

No competing interests declared.

Funding

This work was supported by the National Institute of Health's National Institute of Mental Health (5R21MH112158 to RMH); by the National Institute of General Medical Sciences (R35GM118183 to RH); and by the National Institute on Deafness and Other Communication Disorders (R01DC011901 to RMH). PW was supported by the National Heart, Lung, and Blood Institute (K99HL127275). NS acknowledges funding support from the University of Cyprus and inspiration from the Fulbright Visiting Scholar scheme for an experimental work visit at the Heald and Harland laboratories at UC Berkeley.

Data availability

Full-length *X. tropicalis katnal2* isoforms were submitted to Genbank and can be found under accession MH036373 (larger isoform) and MH036374 (shorter isoform).

Appendix A. Supporting information

Supplementary data associated with this article can be found in the online version at doi:10.1016/j.ydbio.2018.08.002.

References

Antoniades, I., Stylianou, P., Skourides, P.A., 2014. Making the connection: ciliary adhesion complexes anchor basal bodies to the actin cytoskeleton. Dev. Cell 28, 70–80. http://dx.doi.org/10.1016/j.devcel.2013.12.003.

Banks, G., Lassi, G., Hoerder-Suabedissen, A., Tinarelli, F., Simon, M.M., Wilcox, A., Lau, P., Lawson, T.N., Johnson, S., Rutman, A., Sweeting, M., Chesham, J.E., Barnard, A.R., Horner, N., Westerberg, H., Smith, L.B., Molnár, Z., Hastings, M.H., Hirst, R.A., Tucci, V., Nolan, P.M., 2017. A missense mutation in Katnal1 underlies behavioural, neurological and ciliary anomalies. Mol. Psychiatry 9999, 1–10. http://dx.doi.org/10.1038/mp.2017.54.

Bartholdi, D., Stray-Pedersen, A., Azzarello-Burri, S., Kibaek, M., Kirchhoff, M., Oneda, B., Rødningen, O., Schmitt-Mechelke, T., Rauch, A., Kjaergaard, S., 2014. A newly recognized 13q12.3 microdeletion syndrome characterized by intellectual disability, microcephaly, and eczema/atopic dermatitis encompassing the HMGB1and KATNAL1 genes. Am. J. Med. Genet. 164, 1277–1283. http://dx.doi.org/10.1002/ajmg.a.36439.

Bhattacharya, D., Marfo, C.A., Li, D., Lane, M., Khokha, M.K., 2015. CRISPR/Cas9: an inexpensive, efficient loss of function tool to screen human disease genes in Xenopus. Dev. Biol. 408, 196–204. http://dx.doi.org/10.1016/j.ydbio.2015.11.003.

Brooks, E.R., Wallingford, J.B., 2014. Multiciliated cells. Curr. Biol. 24, R973–R982. http://dx.doi.org/10.1016/j.cub.2014.08.047.

Christodoulou, A., Lederer, C.W., Surrey, T., Vernos, I., Santama, N., 2006. Motor protein KIFC5A interacts with Nubp1 and Nubp2, and is implicated in the regulation of centrosome duplication. J. Cell Sci. 119, 2035–2047. http://dx.doi.org/10.1242/jcs.02922.

Dhorne-Pollet, S., Thélie, A., Pollet, N., 2013. Validation of novel reference genes for RT-qPCR studies of gene expression in Xenopus tropicalis during embryonic and post-embryonic development. Dev. Dyn. 242, 709–717. http://dx.doi.org/10.1002/dvdy.23972.

Dunleavy, J.E.M., Okuda, H., O'Connor, A.E., Merriner, D.J., O'Donnell, L., Jamsai, D., Bergmann, M., O'Bryan, M.K., 2017. Katanin-like 2 (KATNAL2) functions in multiple aspects of haploid male germ cell development in the mouse. PLoS Genet. 13, e1007078. http://dx.doi.org/10.1371/journal.pgen.1007078.

Dymek, E.E., Lefebvre, P.A., Smith, E.F., 2004. PF15p is the chlamydomonas homologue of the Katanin p80 subunit and is required for assembly of flagellar central microtubules. Eukaryot. Cell 3, 870–879. http://dx.doi.org/10.1128/EC.3.4.870-879.2004.

Eckert, T., Le, D.T.-V., Link, S., Friedmann, L., Woehlke, G., 2012. Spastin's Microtubule-binding properties and comparison to katanin. PLoS One 7. http://dx.doi.org/10.1371/journal.pone.0050161, e50161–16.

Emes, R.D., Ponting, C.P., 2001. A new sequence motif linking lissencephaly, Treacher Collins and oral-facial-digital type 1 syndromes, microtubule dynamics and cell migration. Hum. Mol. Genet 10, 2813–2820.

Guo, J., Higginbotham, H., Li, J., Nichols, J., Hirt, J., Ghukasyan, V., Anton, E.S., 2015. Developmental disruptions underlying brain abnormalities in ciliopathies. Nat. Commun. 6, 1–13. http://dx.doi.org/10.1038/ncomms8857.

Hartman, J.J., Mahr, J., McNally, K., Okawa, K., Iwamatsu, A., Thomas, S., Cheesman, S., Heuser, J., Vale, R.D., McNally, F.J., 1998. Katanin, a microtubule-severing protein, is a novel AAA ATPase that targets to the centrosome using a WD40-containing subunit. Cell 93, 277–287.

Hartman, J.J., Vale, R.D., 1999. Microtubule disassembly by ATP-dependent oligomerization of the AAA enzyme katanin. Science 286, 782–785.

Heald, R., Nogales, E., 2002. Microtubule dynamics. J. Cell Sci. 115, 3–4.

Hu, W.F., Pomp, O., Ben-Omran, T., Kodani, A., Henke, K., Mochida, G.H., Yu, T.W., Woodworth, M.B., Bonnard, C., Raj, G.S., Tan, T.T., Hamamy, H., Masri, A., Shboul, M., Al-Saffar, M., Partlow, J.N., Al-Dosari, M., Alazami, A., Alowain, M., Alkuraya, F.S., Reiter, J.F., Harris, M.P., Reversade, B., Walsh, C.A., 2014. Katanin p80 regulates human cortical development by limiting centriole and cilia number. Neuron 84, 1240–1257. http://dx.doi.org/10.1016/j.neuron.2014.12.017.

Ioannou, A., Santama, N., Skourides, P.A., 2013. Xenopus laevis nucleotide binding protein 1 (xNubp1) is important for convergent extension movements and controls ciliogenesis via regulation of the actin cytoskeleton. Dev. Biol. 380, 243–258. http://dx.doi.org/10.1016/j.ydbio.2013.05.004.

Iossifov, I., O'Roak, B.J., Sanders, S.J., Ronemus, M., Krumm, N., Levy, D., Stessman, H.A., Witherspoon, K.T., Vives, L., Patterson, K.E., Smith, J.D., Paeper, B., Nickerson, D.A., Dea, J., Dong, S., Gonzalez, L.E., Mandell, J.D., Mane, S.M., Murtha, M.T., Sullivan, C.A., Walker, M.F., Waqar, Z., Wei, L., Willsey, A.J., Yamrom, B., Lee, Y.-H., Grabowska, E., Dalkic, E., Wang, Z., Marks, S., Andrews, P., Leotta, A., Kendall, J., Hakker, I., Rosenbaum, J., Ma, B., Rodgers, L., Troge, J., Narzisi, G., Yoon, S., Schatz, M.C., Ye, K., McCombie, W.R., Shendure, J., Eichler, E.E., State, M.W., Wigler, M., 2014. The contribution of de novo coding mutations to autism spectrum disorder. Nature 515, 216–221. http://dx.doi.org/10.1038/nature13908.

Kapitein, L.C., Hoogenraad, C.C., 2015. Building the neuronal microtubule cytoskeleton. Neuron 87, 492–506. http://dx.doi.org/10.1016/j.neuron.2015.05.046.

Khokha, M.K., Chung, C., Bustamante, E.L., Gaw, L.W.K., Trott, K.A., Yeh, J., Lim, N., Lin, J.C.Y., Taverner, N., Amaya, E., Papalopulu, N., Smith, J.C., Zorn, A.M., Harland, R.M., Grammer, T.C., 2002. Techniques and probes for the study of Xenopus tropicalis development. Dev. Dyn. 225, 499–510. http://dx.doi.org/10.1002/dvdy.10184.

Kypri, E., Christodoulou, A., Maimaris, G., Lethan, M., Markaki, M., Lysandrou, C., Lederer, C.W., Tavernarakis, N., Geimer, S., Pedersen, L.B., Santama, N., 2014. The nucleotide-binding proteins Nubp1 and Nubp2 are negative regulators of ciliogenesis. Cell Mol. Life Sci. 71, 517–538. http://dx.doi.org/10.1007/s00018-013-1401-6.

Loughlin, R., Wilbur, J.D., McNally, F.J., Nédélec, F.J., Heald, R., 2011. Katanin contributes to interspecies spindle length scaling in Xenopus. Cell 147, 1397–1407. http://dx.doi.org/10.1016/j.cell.2011.11.014.

Matis, M., Russler-Germain, D.A., Hu, Q., Tomlin, C.J., Axelrod, J.D., 2014. Microtubules provide directional information for core PCP function. eLife 3, 959–976. http://dx.doi.org/10.7554/eLife.02893.

McNally, F.J., Vale, R.D., 1993. Identification of katanin, an ATPase that severs and disassembles stable microtubules. Cell 75, 419–429.

Mishra-Gorur, K., Cağlayan, A.O., Schaffer, A.E., Chabu, C., Henegariu, O., Vonhoff, F., Akgümüş, G.T., Nishimura, S., Han, W., Tu, S., Baran, B., Gümüş, H., Dilber, C., Zaki, M.S., Hossni, H.A.A., Rivière, J.-B., Kayserili, H., Spencer, E.G., Rosti, R.Ö., Schroth, J., Per, H., Çağlar, C., Çağlar, Ç., Dölen, D., Baranoski, J.F., Kumandaş, S., Minja, F.J., Erson-Omay, E.Z., Mane, S.M., Lifton, R.P., Xu, T., Keshishian, H., Dobyns, W.B., Chi, N.C., Sestan, N., Louvi, A., Bilguvar, K., Yasuno, K., Gleeson, J.G., Gunel, M., 2014. Mutations in KATNB1 cause complex cerebral malformations by disrupting asymmetrically dividing neural progenitors. Neuron 84, 1226–1239. http://dx.doi.org/10.1016/j.neuron.2014.12.014.

Moreno-Mateos, M.A., Vejnar, C.E., Beaudoin, J.-D., Fernandez, J.P., Mis, E.K., Khokha, M.K., Giraldez, A.J., 2015. CRISPRscan: designing highly efficient sgRNAs for CRISPR-Cas9 targeting in vivo. Nat. Methods 12, 982–988. http://dx.doi.org/10.1038/nmeth.3543.

Morin, R.D., Chang, E., Petrescu, A., Liao, N., Griffith, M., Chow, W., Kirkpatrick, R., Butterfield, Y.S., Young, A.C., Stott, J., Barber, S., Babakaiff, R., Dickson, M.C., Matsuo, C., Wong, D., Yang, G.S., Smailus, D.E., Wetherby, K.D., Kwong, P.N., Grimwood, J., Brinkley, C.P., Brown-John, M., Reddix-Dugue, N.D., Mayo, M., Schmutz, J., Beland, J., Park, M., Gibson, S., Olson, T., Bouffard, G.G., Tsai, M., Featherstone, R., Chand, S., Siddiqui, A.S., Jang, W., Lee, E., Klein, S.L., Blakesley, R.W., Zeeberg, B.R., Narasimhan, S., Weinstein, J.N., Pennacchio, C.P., Myers, R.M., Green, E.D., Wagner, L., Gerhard, D.S., Marra, M.A., Jones, S.J.M., Holt, R.A., 2006. Sequencing and analysis of 10,967 full-length cDNA clones from Xenopus laevis and Xenopus tropicalis reveals post-tetraploidization transcriptome remodeling. Genome Res. 16, 796–803. http://dx.doi.org/10.1101/gr.4871006.

Neale, B.M., Kou, Y., Liu, L., Ma'ayan, A., Samocha, K.E., Sabo, A., Lin, C.-F., Stevens, C., Wang, L.-S., Makarov, V., Polak, P., Yoon, S., Maguire, J., Crawford, E.L., Campbell, N.G., Geller, E.T., Valladares, O., Schafer, C., Liu, H., Zhao, T., Cai, G., Lihm, J., Dannenfelser, R., Jabado, O., Peralta, Z., Nagaswamy, U., Muzny, D., Reid, J.G., Newsham, I., Wu, Y., Lewis, L., Han, Y., Voight, B.F., Lim, E., Rossin, E., Kirby, A., Flannick, J., Fromer, M., Shakir, K., Fennell, T., Garimella, K., Banks, E., Poplin, R.,

Gabriel, S., dePristo, M., Wimbish, J.R., Boone, B.E., Levy, S.E., Betancur, C., Sunyaev, S., Boerwinkle, E., Buxbaum, J.D., Cook, E.H., Devlin, B., Gibbs, R.A., Roeder, K., Schellenberg, G.D., Sutcliffe, J.S., Daly, M.J., 2012. Patterns and rates of exonic de novo mutations in autism spectrum disorders. Nature 485, 242–245. http://dx.doi.org/10.1038/nature11011.

Nieuwkoop, P.D., Faber, J., 1994. Normal Table of Xenopus laevis (Daudin). Garland Publishing, New York.

O'Roak, B.J., Vives, L., Girirajan, S., Karakoc, E., Krumm, N., Coe, B.P., Levy, R., Ko, A., Lee, C., Smith, J.D., Turner, E.H., Stanaway, I.B., Vernot, B., Malig, M., Baker, C., Reilly, B., Akey, J.M., Borenstein, E., Rieder, M.J., Nickerson, D.A., Bernier, R., Shendure, J., Eichler, E.E., 2012. Sporadic autism exomes reveal a highly interconnected protein network of de novo mutations. Nature 485, 246–250. http://dx.doi.org/10.1038/nature10989.

Parikshak, N.N., Luo, R., Zhang, A., Won, H., Lowe, J.K., Chandran, V., Horvath, S., Geschwind, D.H., 2013. Integrative functional genomic analyses implicate specific molecular pathways and circuits in autism. Cell 155, 1008–1021. http://dx.doi.org/10.1016/j.cell.2013.10.031.

Park, T.J., Mitchell, B.J., Abitua, P.B., Kintner, C., Wallingford, J.B., 2008. Dishevelled controls apical docking and planar polarization of basal bodies in ciliated epithelial cells. Nat. Genet. 40, 871–879. http://dx.doi.org/10.1038/ng.104.

Roll-Mecak, A., McNally, F.J., 2010. Microtubule-severing enzymes. Curr. Opin. Cell Biol. 22, 96–103. http://dx.doi.org/10.1016/j.ceb.2009.11.001.

Sanders, S.J., He, X., Willsey, A.J., Ercan-Sencicek, A.G., Samocha, K.E., Cicek, A.E., Murtha, M.T., Bal, V.H., Bishop, S.L., Dong, S., Goldberg, A.P., Jinlu, C., Keaney, J.F., III, Klei, L., Mandell, J.D., Moreno-De-Luca, D., Poultney, C.S., Robinson, E.B., Smith, L., Solli-Nowlan, T., Su, M.Y., Teran, N.A., Walker, M.F., Werling, D.M., Beaudet, A.L., Cantor, R.M., Fombonne, E., Geschwind, D.H., Grice, D.E., Lord, C., Lowe, J.K., Mane, S.M., Martin, D.M., Morrow, E.M., Talkowski, M.E., Sutcliffe, J.S., Walsh, C.A., Yu, T.W., Ledbetter, D.H., Martin, C.L., Cook, E.H., Buxbaum, J.D., Daly, M.J., Devlin, B., Roeder, K., State, M.W., Consortium, A.S., 2015. Insights into autism spectrum disorder genomic architecture and biology from 71 risk loci. Neuron 87, 1215–1233. http://dx.doi.org/10.1016/j.neuron.2015.09.016.

Sanders, S.J., Murtha, M.T., Gupta, A.R., Murdoch, J.D., Raubeson, M.J., Willsey, A.J., Ercan-Sencicek, A.G., DiLullo, N.M., Parikshak, N.N., Stein, J.L., Walker, M.F., Ober, G.T., Teran, N.A., Song, Y., El-Fishawy, P., Murtha, R.C., Choi, M., Overton, J.D., Bjornson, R.D., Carriero, N.J., Meyer, K.A., Bilguvar, K., Mane, S.M., Sestan, N., Lifton, R.P., Gunel, M., Roeder, K., Geschwind, D.H., Devlin, B., State, M.W., 2012. De novo mutations revealed by whole-exome sequencing are strongly associated with autism. Nature 485, 237–241. http://dx.doi.org/10.1038/nature10945.

Schweickert, A., Feistel, K., 2015. The Xenopus embryo: an ideal model system to study human ciliopathies. Curr. Pathobiol. Rep. 3, 115–127. http://dx.doi.org/10.1007/s40139-015-0074-2.

Sharma, N., Bryant, J., Wloga, D., Donaldson, R., Davis, R.C., Jerka-Dziadosz, M., Gaertig, J., 2007. Katanin regulates dynamics of microtubules and biogenesis of motile cilia. J. Cell Biol. 178, 1065–1079. http://dx.doi.org/10.1083/jcb.200704021.

Sive, H.L., Grainger, R.M., Harland, R.M., 2000. Early Development of Xenopus laevis: A Laboratory Manual. Cold Spring Harbor Laboratory Press, Cold Spring Harbor, New York.

Stessman, H.A.F., Xiong, B., Coe, B.P., Wang, T., Hoekzema, K., Fenckova, M., Kvarnung, M., Gerdts, J., Trinh, S., Cosemans, N., Vives, L., Lin, J., Turner, T.N., Santen, G., Ruivenkamp, C., Kriek, M., van Haeringen, A., Aten, E., Friend, K., Liebelt, J., Barnett, C., Haan, E., Shaw, M., Gecz, J., Anderlid, B.-M., Nordgren, A., Lindstrand, A., Schwartz, C., Kooy, R.F., Vandeweyer, G., Helsmoortel, C., Romano, C., Alberti, A., Vinci, M., Avola, E., Giusto, S., Courchesne, E., Pramparo, T., Pierce, K., Nalabolu, S., Amaral, D.G., Scheffer, I.E., Delatycki, M.B., Lockhart, P.J., Hormozdiari, F., Harich, B., Castells-Nobau, A., Xia, K., Peeters, H., Nordenskjöld, M., Schenck, A., Bernier, R.A., Eichler, E.E., 2017. Targeted sequencing identifies 91 neurodevelopmental- disorder risk genes with autism and developmental-disability biases. Nat. Genet. 49, 515–526. http://dx.doi.org/10.1038/ng.3792.

Tu, F., Sedzinski, J., Ma, Y., Marcotte, E.M., Wallingford, J.B., 2018. Protein localization screening in vivo reveals novel regulators of multiciliated cell development and function. J. Cell Sci., 131. http://dx.doi.org/10.1242/jcs.206565.

Ververis, A., Christodoulou, A., Christoforou, M., Kamilari, C., Lederer, C.W., Santama, N., 2016. A novel family of katanin-like 2 protein isoforms (KATNAL2), interacting with nucleotide-binding proteins Nubp1 and Nubp2, are key regulators of different MT-based processes in mammalian cells. Cell Mol. Life Sci. 73, 163–184. http://dx.doi.org/10.1007/s00018-015-1980-5.

Walentek, P., Quigley, I.K., 2017. What we can learn from a tadpole about ciliopathies and airway diseases: using systems biology in Xenopus to study cilia and mucociliary epithelia. Genesis 55. http://dx.doi.org/10.1002/dvg.23001, (e23001–12).

Walentek, P., Quigley, I.K., Sun, D.I., Sajjan, U.K., Kintner, C., Harland, R.M., 2016. Ciliary transcription factors and miRNAs precisely regulate Cp110 levels required for ciliary adhesions and ciliogenesis. eLife 5, 70. http://dx.doi.org/10.7554/eLife.17557.

Wallingford, J.B., Mitchell, B., 2011. Strange as it may seem: the many links between Wnt signaling, planar cell polarity, and cilia. Genes Dev. 25, 201–213. http://dx.doi.org/10.1101/gad.2008011.

Williams, M.R., Fricano-Kugler, C.J., Getz, S.A., Skelton, P.D., Lee, J., Rizzuto, C.P., Geller, J.S., Li, M., Luikart, B.W., 2016. A retroviral CRISPR-Cas9 system for cellular autism-associated phenotype discovery in developing neurons. Sci. Rep. 6, 1–11. http://dx.doi.org/10.1038/srep25611.

Willsey, A.J., Sanders, S.J., Li, M., Dong, S., Tebbenkamp, A.T., Muhle, R.A., Reilly, S.K., Lin, L., Fertuzinhos, S., Miller, J.A., Murtha, M.T., Bichsel, C., Niu, W., Cotney, J., Ercan-Sencicek, A.G., Gockley, J., Gupta, A.R., Han, W., He, X., Hoffman, E.J., Klei, L., Lei, J., Liu, W., Liu, L., Lu, C., Xu, X., Zhu, Y., Mane, S.M., Lein, E.S., Wei, L., Noonan, J.P., Roeder, K., Devlin, B., Sestan, N., State, M.W., 2013. Coexpression networks implicate human midfetal deep cortical projection neurons in the pathogenesis of autism. Cell 155, 997–1007. http://dx.doi.org/10.1016/j.cell.2013.10.020.

Yang, Z., Steentoft, C., Hauge, C., Hansen, L., Thomsen, A.L., Niola, F., Vester-Christensen, M.B., Frödin, M., Clausen, H., Wandall, H.H., Bennett, E.P., 2015. Fast and sensitive detection of indels induced by precise gene targeting. Nucleic Acids Res. 43, e59. http://dx.doi.org/10.1093/nar/gkv126.